Frontiers of Information Technology & Electronic Engineering
www.jzus.zju.edu.cn; engineering.cae.cn; www.springerlink.com
ISSN 2095-9184 (print); ISSN 2095-9230 (online)
E-mail: jzus@zju.edu.cn

Correspondence:

Analysis of spatial power synthesis efficiency based on the near-field cross-beam theory for distributed UAV interference applications*

Dalong XU[†1], Jian WU[1,2], Jianyin CAO[†‡1], Hao WANG[1,2], Xiang LI[2]

[1]*School of Electronic and Optical Engineering, Nanjing University of Science and Technology, Nanjing 210094, China*

[2]*Nanhu Laboratory, Jiaxing 314050, China*

[†]E-mail: xudl1987@njust.edu.cn; jianyin.cao@njust.edu.cn

Received May 16, 2024; Revision accepted Aug. 12, 2024; Crosschecked Oct. 24, 2024

https://doi.org/10.1631/FITEE.2400401

This paper discusses a novel method for calculating near-field spatial power synthesis efficiency based on the cross-beam synthesis theory for the application of unmanned aerial vehicle (UAV) swarms in electronic countermeasure systems. The model of a UAV array and the working principle of the near-field spatial power synthesis are used to explain the power synthesis efficiency of UAV interference. The influence of location parameters, such as the positioning and attitude accuracy of UAVs, is analyzed. The influences of UAVs in actual situations, including the jitter of platforms, damage rate, and time synchronization accuracy in real conditions, are also analyzed. Finally, a test scenario based on fiber-optic synchronization is constructed to measure the spatial power synthesis efficiency with high-precision time synchronization. The results provide further evidence of the effectiveness and reliability of the proposed near-field cross-beam calculation method for distributed UAV interference applications.

1 Introduction

Since the 1920s, the application of UAVs in electronic warfare has developed rapidly, owing to their advantages in avoiding the sacrifice of personnel. The UAV platform has reduced weight and size, robustness, outstanding mission efficacy, and a low cost–effectiveness ratio. In addition, advantages such as high concealment, easy takeoff and landing, simple operation, and flexible maneuverability are attractive (Zhang YX et al., 2017). Since the 1980s, UAVs have played an important role in coordinated combat with manned aircraft and other weapons and have been especially successfully applied in electronic warfare drones in the Gulf War. This has promoted countries around the world to become deeply aware of the enormous importance of electronic warfare drones for high-tech local wars, and they are irreplaceable with other methods (Luo, 2009).

Nowadays, the demand for small, highly maneuverable jamming systems has increased in response to a variety of interference targets and complex environments. Because of this, intelligent “swarm” technologies formed of arrays of payload-equipped UAVs have emerged as a research hotspot. However, UAV platforms have limitations in terms of the carrying capacity,

‡ Corresponding author

* Project supported by the Youth Foundation of Jiangsu Province, China (No. BK20230919)

ORCID: Dalong XU, https://orcid.org/0009-0005-1410-5369; Jianyin CAO, https://orcid.org/0009-0008-4226-422X

since high maneuverability is required. High-power radar systems are hardly to be carried by the UAV platforms, leading to insufficient damage power for jamming. Thus, multiple drones need to be used as subarrays to form a larger array to improve damage power.

Spatial power synthesis technology has been developed to use multiple payload units that emit electromagnetic waves with the same frequency and a specific phase relationship to form high-power electromagnetic beams in a certain direction (Liu SD et al., 2006). Zhang YB et al. (2006) introduced a method for calculating spatial power synthesis efficiency concerning phase differences between signals. Based on this foundation, research on spatial power synthesis technology and factors affecting synthesis efficiency has been conducted.

Liu W et al. (2012) simplified the expression of spatial power synthesis efficiency and analyzed the impact of amplitude difference and phase difference between signals. Xu et al. (2013) obtained an analytical expression for the expected synthesis efficiency of arbitrary microwave sources, and analyzed three typical random phase error distributions. Yao et al. (2015) studied the relationship between the average system gain and the number of array elements, as well as the amplitude difference and phase difference of each unit. In Zhang K et al. (2016) and Ju et al. (2020), these theories were applied to the analysis of spatial synthesis efficiency in multiple interference jammer scenarios. However, both the theoretical derivation and practical application of these studies employ the method of parallel-beam synthesis when the target is in a far-field region of the array.

When the targets for UAV swarms flying at low altitudes are located in the near-field region, the aforementioned calculation methods become inaccurate. The work by Kennedy et al. (1998), Chen et al. (2015), Cicchetti et al. (2019), and Tian (2019) qualitatively analyzed the distribution of efficiency in the target area, which is located in the near-field region of the array. Based on the concept and principle of sparse array coherent signal power synthesis, Chen et al. (2015) researched the method of cross-beam synthesis to derive and analyze the relationship between the cross angle of beams and target point synthesis efficiency under two-point source cross-beams. This paper also proposed a phase compensation method and eliminated the influence of unit directional patterns on synthesis efficiency. Tian (2019) established a distributed fixed array near-field power synthesis mathematical model based on time inversion and quantitatively analyzed the error factors that affect the synthesis effect.

However, these situations are ideal, and the number of research units is relatively small in the above studies. A comprehensive analysis of the factors influencing the synthesis efficiency at target points is still lacking, as is the experimental verification. To address these issues, this paper combines power synthesis technology in free space with the theory of cross-beam synthesis. Spatial power synthesis efficiency at a specified near-field point is further analyzed based on the previous work (Wu et al., 2023). A comparison of the proposed method with traditional far-field calculation methods is conducted. The impact of parameters such as UAV positioning accuracy, attitude accuracy, time synchronization accuracy, and failure rate are also analyzed. Finally, a test scenario with time synchronization is designed, and spatial power synthesis efficiency is measured to provide experimental evidence for the proposed computational method.

2 Principle of spatial power synthesis based on the cross-beam theory

The common rule of thumb for the approximate distance at which the far-field approximation begins to be valid is $r=2D^2/\lambda$ (Kennedy et al., 1998). For array antennas, D represents the aperture of the antenna array, and λ represents the wavelength. The schematic of UAVs simultaneously interfering with the target is shown in Fig.1. Due to the low altitude of UAV flight

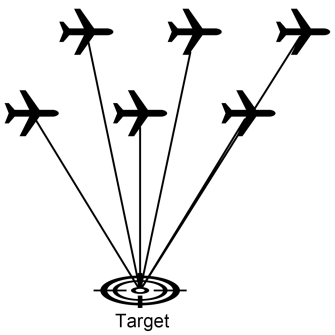

Fig. 1 Schematic of unmanned aerial vehicle (UAV) interference with the target

typically within a few kilometers and the inter-element spacing of the distributed array usually being more than 10 wavelengths, the interference target is considered to be in the near field of the distributed array. Therefore, the method of cross-beam spatial power synthesis is discussed in this paper.

The model of distributed power synthesis is shown in Fig. 2; the target point is considered as the origin of the coordinate system, and the position of UAV i is denoted as (R_i, ϕ_i, θ_i) (i=0, 1, ⋯, N−1). R_i represents the distance from the target to UAV i. Assume that the electric field intensity generated by UAV i at the target point is denoted as E_i. According to the antenna radiation and electromagnetic wave propagation theory, E_i can be calculated by

$$E_i = \Delta_c \frac{f_i(\theta_i,\phi_i)}{|R_i|^2} C_i e^{-j(kR_i-\varphi_i)}, \tag{1}$$

where f_i represents the active far-field radiation pattern of UAV i, k=2π/λ, φ_i represents the initial phase of signal i, and Δ_c could be regarded as a constant. C_i represents the attenuation constant caused by adverse environmental factors such as rain and heavy fog. For each individual element, the target is still considered in the far-field region. When deploying a sparse array configuration, the mutual coupling between elements can be neglected, as the spacing between elements is much larger than the operating wavelength. Therefore, the passive element radiation pattern can be used as a substitute.

To maximize spatial synthesis efficiency, it is necessary to perform pre-compensation processing on the initial phase of each unit signal, so that the phases of all signals reaching the target location are the same. The initial phase of signal i is calculated as

$$\varphi_i = kR_i - \varphi_0, \tag{2}$$

where φ_0 represents the initial phase of the signal when i=0.

The phase of each signal reaching the target location is

$$\phi_i = -kR_i + \varphi_i = \varphi_0 + \delta_i, \tag{3}$$

where δ_i represents the difference of UAV i relative to the ideal situation.

Since the interference target is located in the near field of the antenna array, the electric field does not satisfy the condition of co-directional superposition. Therefore, the electric field should be decomposed into three axes, x, y, and z. The decomposed electric field is obtained as

$$\begin{cases} E_{ix} = \Delta_c \dfrac{f_i(\theta_i,\phi_i)}{R_i} \cos(\theta_i)\cos(\phi_i) e^{-(\varphi_0-\delta_i)}, \\ E_{iy} = \Delta_c \dfrac{f_i(\theta_i,\phi_i)}{R_i} \cos(\theta_i)\sin(\phi_i) e^{-(\varphi_0-\delta_i)}, \\ E_{iz} = \Delta_c \dfrac{f_i(\theta_i,\phi_i)}{R_i} \sin(\theta_i) e^{-(\varphi_0-\delta_i)}, \end{cases} \tag{4}$$

where E_{ix}, E_{iy}, and E_{iz} represent each element's electric field along the x, y, and z axes at the target point, respectively. The composite field strength is given by

$$\begin{aligned} |E|^2 &= \left|\sum_{i=1}^{N} E_{ix}\right|^2 + \left|\sum_{i=1}^{N} E_{iy}\right|^2 + \left|\sum_{i=1}^{N} E_{iz}\right|^2 \\ &= \sum_{i=0}^{N-1}\left(\frac{f_i(\theta_i,\phi_i)}{R_i}\right)^2 + \sum_{i=0}^{N-2}\sum_{j=i+1}^{N-1}\left[\frac{f_i(\theta_i,\phi_i)}{R_i}\frac{f_j(\theta_j,\phi_j)}{R_j}\right. \\ &\left.\cdot\cos(\delta_i-\delta_j)\left(\cos\theta_i\cos\theta_j\cos(\phi_i-\phi_j)+\sin\theta_i\sin\theta_j\right)\right]. \end{aligned} \tag{5}$$

The spatial power synthesis efficiency is defined as the ratio of the power density at the target point to the maximum power density at the target point. It can be expressed as

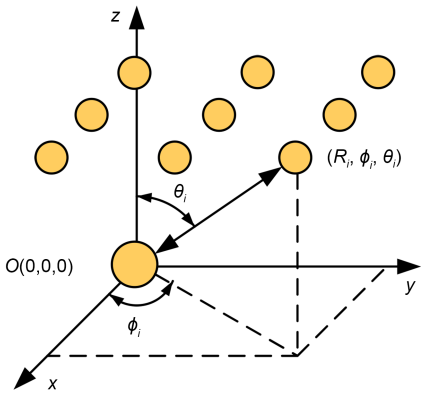

Fig. 2 Model of the distributed power synthesis

$$\eta_{\text{cross}}=\frac{P_{\text{R}}}{P_{\text{R max}}}=\frac{|E|^2}{|E_{\max}|^2}=\sum_{i=0}^{N-1}\left(\frac{f_i(\theta_i,\phi_i)}{R_i}\right)^2 +\frac{1}{N^2}\sum_{i=0}^{N-2}\sum_{j=i+1}^{N-1}\left[\frac{f_i(\theta_i,\phi_i)}{R_i}\frac{f_j(\theta_j,\phi_j)}{R_j}\cos(\delta_i-\delta_j)\cdot\left(\cos\theta_i\cos\theta_j\cos(\phi_i-\phi_j)+\sin\theta_i\sin\theta_j\right)\right]. \quad (6)$$

Substituting $\theta_i=\theta_j$ and $\phi_i=\phi_j$ into Eq. (6), the expression under parallel-beam synthesis is shown as

$$\eta_{\text{parallel}}=\frac{1}{N^2}\left[\sum_{i=0}^{N-1}\left(\frac{f_i(\theta_i,\phi_i)}{R_i}\right)^2 +\sum_{i=0}^{N-2}\sum_{j=i+1}^{N-1}\left(\frac{f_i(\theta_i,\phi_i)}{R_i}\frac{f_j(\theta_j,\phi_j)}{R_j}\cos(\delta_i-\delta_j)\right)\right]. \quad (7)$$

3 Analysis of factors impacting spatial power synthesis

3.1 Simulated model for UAV position deviation

The effects of several key factors on spatial synthesis efficiency, including payload carrier frequency, beam width, positioning error, attitude error, and UAV failure rate, are investigated based on Eq. (6). The simulation results under parallel-beam synthesis are compared based on Eq. (7).

As depicted in Fig. 3, the range of UAV shaking is represented by (Δx, Δy, Δz), and the coordinates of the UAVs are denoted as (Δx, id+Δy, H+Δz). To quantify the impact of shaking on the system, the wavefront error Δd and the phase error δ are calculated as

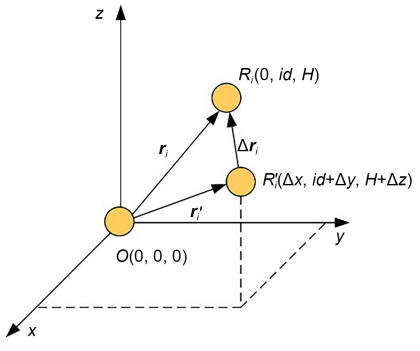

Fig. 3 Simulated model for the UAV position deviation

$$\delta = 2\pi f\Delta d/c, \quad (8)$$

where c is the propagation speed of electromagnetic waves in the free space.

Assume that the elevation angle of UAV i relative to the target point in the ideal state is θ_i, and that the azimuth angle is represented as ϕ_i. The elevation angle and azimuth angle of UAV i are relative to the target point after shaking as θ_i' and ϕ_i', respectively.

To analyze the effects caused by positioning and attitude errors, σ_{pa} is defined to represent the positioning accuracy, where $\Delta x=\Delta y=\Delta z=\sigma_{\text{pa}}$. Similarly, σ_{aa} is defined to represent the attitude accuracy, where $\Delta\theta_i'=\Delta\phi_i'=\sigma_{\text{aa}}$. In the simulation, 100 000 sets of positioning errors satisfying a uniform distribution $U(-\sigma_{\text{pa}}/2, \sigma_{\text{pa}}/2)$, 100 000 sets of attitude errors satisfying a uniform distribution $U(-\sigma_{\text{aa}}/2, \sigma_{\text{aa}}/2)$, and 100 000 sets of time synchronization errors satisfying a uniform distribution $U(0, \sigma_{\text{tsa}}/2)$ are applied. Each set of errors will be considered separately to analyze the power synthesis efficiency. To assess the synthesis efficiency under the given positioning or attitude error conditions, the average of the power synthesis efficiencies across all 100 000 scenarios is calculated. The default parameters for the simulation analysis are outlined in Table 1. These parameters provide a consistent framework for comparing the effects of different error scenarios.

Table 1 Default parameters used in the simulations

Parameter	Value	Parameter	Value
f (GHz)	2	N	10
σ_{pa} (cm)	3	p_{d} (%)	0
σ_{aa} (°)	3	γ (%)	60
h (m)	500	Θ (°)	60
d (m)	80	σ_{tsa} (ps)	0

p_{d}: probability of damage; γ: threshold for effective synthesis efficiency; Θ: beam width

3.2 Simulated results and analysis

The analysis was set up based on the Matlab software. The relationship between the average synthesis efficiency with the positioning and attitude accuracy was simulated and is shown in Fig. 4. It is evident that there is a rapid decrease in the spatial synthesis efficiency when the positioning error increases. The average synthesis efficiency drops to 60% since the error range reaches 0.056 m. This means that precise positioning accuracy is crucial for achieving effective interference

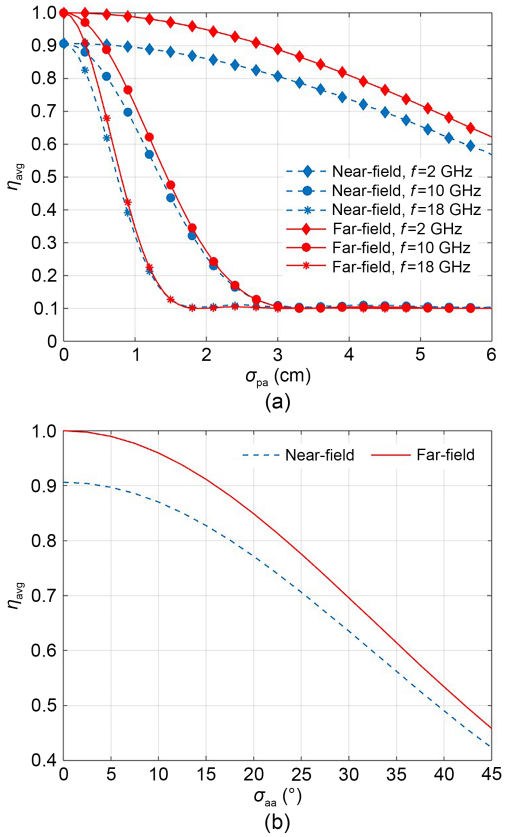

Fig. 4 Relationship between the average synthesis efficiency with positioning accuracy (a) and attitude accuracy (b)

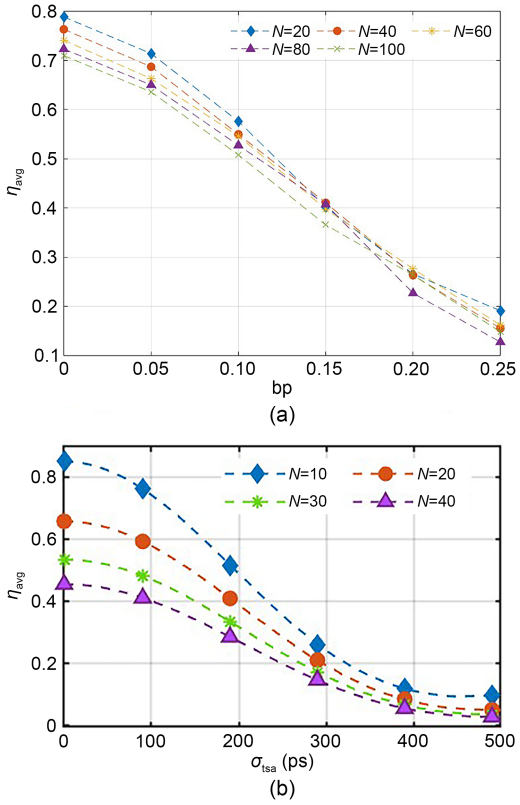

Fig. 5 Relationship between the average synthesis efficiency with UAV damage rate (a) and time synchronization accuracy (b) in the near field accuracy

in the near-field scenario. In Fig. 4b, the average synthesis efficiency of the distributed array decreases as the attitude accuracy errors increase. This highlights the importance of precise attitude accuracy in achieving optimal power synthesis performance.

In addition to the power synthesis efficiency, it is crucial to account for the potential damage inflicted on UAVs during the interference process. The $N\times p_d$ units from a pool of N units are selected as the damaged UAVs, where each damaged UAV is represented as f_i=0. The relationship between the UAV failure rate and the average synthesis efficiency is shown in Fig. 5a. bp is the damage rate of UAVs. The results indicate that the damage rate should be kept lower than 0.06 for a synthesis efficiency of over 60%.

The phase synchronization accuracy between array elements and the time synchronization accuracy are also important factors that affect the spatial power synthesis efficiency. The relationship between the phase synchronization error and the time synchronization error is given by

$$\Delta\delta = 2\pi f\Delta t. \tag{9}$$

Therefore, the impact of time synchronization accuracy on different array numbers is specifically analyzed and is shown in Fig. 5b. The curve shows a relatively flat trend for small and large time differences. However, when the time synchronization accuracy is around 250 ps, a rapid decrease in the average synthesis efficiency happens. Additionally, under the same time synchronization accuracy, the average synthesis efficiency tends to decrease when the number of array elements increases.

In real scenarios, multiple errors coexist simultaneously. However, the impact of damaged UAVs on average synthesis efficiency can be mitigated by replacing them with new UAVs. Additionally, when the beam width is relatively wide, the influence of attitude error is minimal. Thus, time synchronization error and positioning error are the most important factors; their combined effect is shown in Fig. 6. For example, if an average synthesis efficiency of 60% is achieved,

a positioning accuracy within 0.056 m and a time accuracy within 160 ps are required in such near-field beamforming conditions.

4 Experimental testing of near-field beam synthesis efficiency in ideal conditions

Based on the analysis above, an experimental design was developed to investigate the synthesis efficiency with a high time synchronization accuracy and tiny positioning error. The schematic of the test is shown in Fig. 7. Four nodes were used for actual verification, with three nodes as the transmitting end and one node as the receiving end. A higher time synchronization accuracy was made possible by fiber optic. Limited by the test equipment, the payloads were fixed with controllable positioning errors in the experiment. The payloads were equipped with planar spiral antennas as the transmitting end and a planar spiral antenna as the receiving end. The signal processing system and the other components were packaged in the payload. The other equipment included a signal source, a direct current (DC) power supply, a spectrum analyzer, and a 1-m-long fiber-optic cable. The experimental validation was conducted using the schematic shown in Fig. 8.

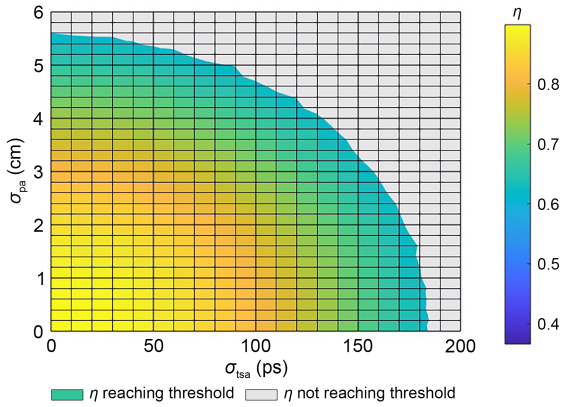

Fig. 6 Relationship between the average synthesis efficiency and time synchronization, as well as positioning accuracy

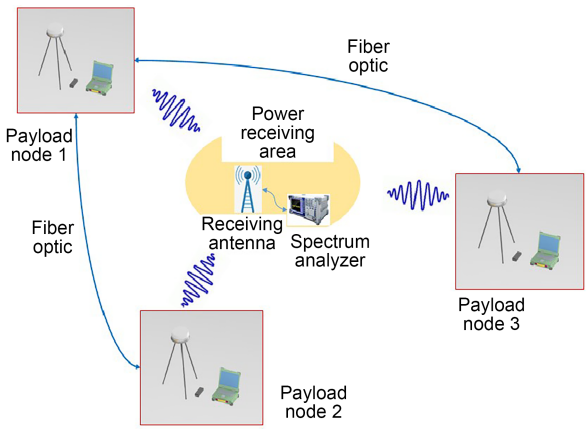

Fig. 7 Test schematic

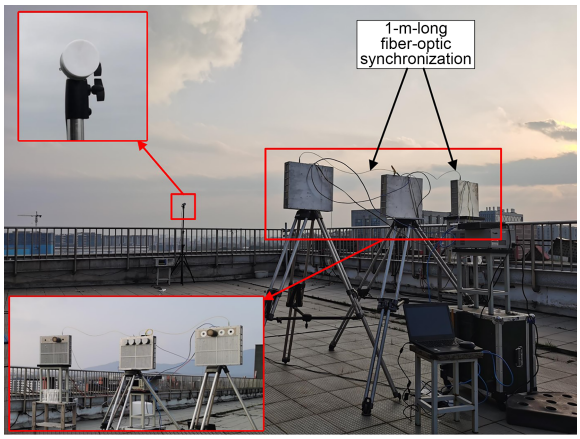

Fig. 8 Test environment setup

Based on the analysis, the spatial power synthesis under short fiber-optic synchronization was tested as follows: First, a test of the power received by the receiving node was performed when only one transmitting node was turned on. Next, the other two nodes were opened and the power received by the receiving end node was tested. In ideal conditions, if the input power of each unit is the same, the electric field strength added at the receiving end will double for each additional node added. When all three nodes are simultaneously activated, the electric field strength at the receiving end is three times that of a single node, resulting in an increase of 9.5 dB in power. Thus, the spatial power synthesis efficiency is calculated as the ratio of the measured value to 9.5 dB in this paper.

The measured power synthesis efficiency and simulations based on near-field cross-beam synthesis are presented in Fig. 9. It becomes apparent that the disparities between the measured and simulated results gradually increase as the frequency increases. Additionally, the impact of positioning error on the test platform is larger than that in the simulation, resulting in a lower power synthesis efficiency in the experimental measurements. Apart from this, the tested efficiency has the same tendency as the simulated

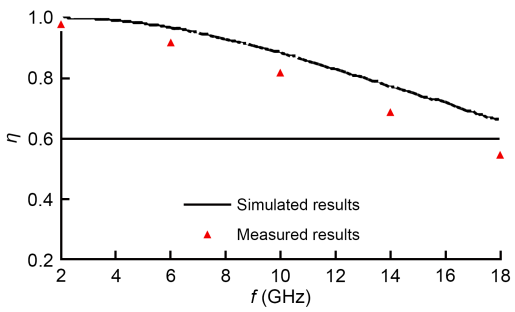

Fig. 9 Measured and simulated power synthesis efficiency

results based on the proposed calculation method. The reliability of the cross-beam synthesis method is verified through the proposed experiments. Compared to the work in Tian (2019), the power synthesis is more focused, and the impact factors are mostly focused on the UAV platform. Although the research on the UAV platform lacks sufficient experimental verification, with the development of UAV platforms and lightweight airborne equipment, this study can still provide some theoretical guidance for the application of UAV swarms in the field of electronic warfare.

5 Conclusions

In this paper, the UAV swarm scenarios were modeled to analyze the impact of performance parameters of UAV platforms and their payloads on the spatial power synthesis efficiency. Specifically focusing on the near-field conditions, the synthesis efficiency was analyzed and tested. The average synthesis efficiency of distributed arrays decreases significantly with the increasing errors, particularly at higher operating frequencies. The impact of attitude accuracy on the average synthesis efficiency is relatively minor compared to the positioning accuracy and time synchronization accuracy. An experiment was designed and measured to validate the reliability of the cross-beam synthesis method. The study in this paper provides a theoretical basis for the layout of low-altitude UAV interference systems and ultimately the improvement of interference efficiency at a certain point.

Contributors

Dalong XU designed the research. Dalong XU, Jian WU, and Jianyin CAO processed the data. Jian WU drafted the paper. Jianyin CAO helped organize the paper. Hao WANG and Xiang LI revised and finalized the paper.

Conflict of interest

All the authors declare that they have no conflict of interest.

Data availability

The data that support the findings of this study are available from the corresponding author upon reasonable request.

References

Chen QJ, Huang WJ, Jiang QX, et al., 2015. Effect of cross angles on power synthesis of cross beams. *Radar Sci Technol*, 13(4):439-443, 448 (in Chinese). https://doi.org/10.3969/j.issn.1672-2337.2015.04.018

Cicchetti R, Faraone A, Testa O, 2019. Near field synthesis based on multi-port antenna radiation matrix eigenfields. *IEEE Access*, 7:62184-62197. https://doi.org/10.1109/ACCESS.2019.2912305

Ju T, Huang GM, Man X, 2020. A spatial power synthetic method for random distributed array communication jammers. *Fire Contr Command Contr*, 45(8):57-61, 67 (in Chinese). https://doi.org/10.3969/j.issn.1002-0640.2020.08.009

Kennedy RA, Abhayapala TD, Ward DB, 1998. Broadband nearfield beamforming using a radial beampattern transformation. *IEEE Trans Signal Process*, 46(8):2147-2156. https://doi.org/10.1109/78.705426

Liu SD, Jiao YC, Zhang FS, 2006. Effect of random surface errors on radiation characteristics of the side-fed offset Cassegrain antenna. *Front Elect Electron Eng China*, 1(3): 345-349. https://doi.org/10.1007/s11460-006-0029-9

Liu W, Zhou HJ, Luo XG, 2012. Combined efficiency analysis of spatial power combining. IEEE 11th Int Conf on Signal Processing, p.333-337. https://doi.org/10.1109/ICoSP.2012.6491668

Luo SG, 2009. Development status and trend of electronic warfare unmanned aerial vehicle. *Shipboard Electron Counterm*, 32(2):26-28, 52 (in Chinese). https://doi.org/10.3969/j.issn.1673-9167.2009.02.006

Tian SY, 2019. Research on Spatial Power Combination Technology of Distributed Array Based on Time Reversal. MS Thesis, National University of Defense Technology, Changsha, China (in Chinese). https://doi.org/10.27052/d.cnki.gzjgu.2019.000835

Wu J, Cao JY, Xu DL, et al., 2023. Analysis of spatial power synthesis based on near-field beamforming theory for distributed UAV interference applications. IEEE 11th Asia-Pacific Conf on Antennas and Propagation, p.1-2. https://doi.org/10.1109/APCAP59480.2023.10470333

Xu G, Xu Y, Shi MY, et al., 2013. Impact of random phase error on microwave power combining efficiency. *High Power Laser Part Beams*, 25(11):2914-2918 (in Chinese). https://doi.org/10.3788/HPLPB20132511.2914

Yao SF, Chu FH, Qu Y, et al., 2015. Analysis about factors

affect spatial power combining efficiency. *Fire Contr Command Contr*, 40(11):77-79 (in Chinese). https://doi.org/10.3969/j.issn.1002-0640.2015.11.017

Zhang K, Liu ZJ, Nie JW, et al., 2016. Spatial power combining based on distributed antennas in Earth station. *Acta Aeronaut Astronaut Sin*, 37(6):1912-1920 (in Chinese). https://doi.org/10.7527/S1000-6893.2016.0001

Zhang YB, Zhang H, Liao GS, 2006. A technology of spatial power-combination for the random decentralized jammer array. *J Xidian Univ*, 33(1):150-155 (in Chinese). https://doi.org/10.3969/j.issn.1001-2400.2006.01.035

Zhang YX, Zeng QD, Zhang W, 2017. Overview of UAV development. *J Henan Sci Technol*, (9):58-59 (in Chinese). https://doi.org/10.3969/j.issn.1003-5168.2017.09.030